PHYSICAL REVIEW B **87**, 041408(R) (2013)

Hybrid electronic-photonic subwavelength cavities operating at terahertz frequencies

E. Strupiechonski,[1] G. Xu,[1] P. Cavalié,[2] N. Isac,[1] S. Dhillon,[2] J. Tignon,[2] G. Beaudoin,[3] I. Sagnes,[3] A. Degiron,[1,*] and R. Colombelli[1,†]

[1]*Institut d'Electronique Fondamentale, Université Paris Sud and CNRS, UMR8622, 91405 Orsay, France*

[2]*Laboratoire Pierre Aigrain, Ecole Normale Supérieure, CNRS (UMR 8551), Université P. et M. Curie, Université D. Diderot, 75231 Paris Cedex 05, France*

[3]*Laboratoire de Photonique et Nanostructures, CNRS UPR20, 91460 Marcoussis, France*

(Received 18 September 2012; revised manuscript received 11 January 2013; published 31 January 2013)

We report on the concept and realization of terahertz (THz) metallic/semiconductor cavities characterized by dimensions as small as $\lambda_{\text{eff}}/9$ in all directions of space (or $\lambda/30$ with the vacuum wavelength). We experimentally prove that the capacitance and inductance of these devices are not interdependent, as in purely photonic cavities, but that they can be adjusted almost independently, as in an electronic circuit. This functionality proves that the dimensions of these hybrid electronic-photonic devices are intrinsically not limited by diffraction as in conventional photonic resonators. Using arguments from transmission line theory, we show that it is necessary to include at least one metallic loop in the cavity design to access this regime and we note, as a corollary, that some recent proposals to miniaturize THz resonators and devices beyond the diffraction limit do not meet this fundamental requirement. Our results shed a light on the ability to describe THz/metallic cavities in terms of circuit elements. Furthermore, upon insertion of electrical contacts, these extremely subwavelength resonators can potentially lead to advances in THz detectors and phased array antennas.

DOI: 10.1103/PhysRevB.87.041408 PACS number(s): 42.79.Gn, 03.50.De, 81.16.−c

Metallic resonators are ubiquitous in THz photonics owing to their central role in metamaterials,[1,2] intersubband-transitions based devices operating in both weak- and strong-coupling regimes,[3–5] and antennas for sensors and sources.[6,7] Since metallic resonators carry a real electronic current, their size is not always constrained by the diffraction limit. Indeed some designs such as split ring resonators[8] and derivatives[1–3] can be considered as resonant circuits defined by an inductance L and a capacitance C (LC resonators). THz LC resonators, however, rely in general on planar geometries as current fabrication techniques are optimized for two-dimensional (2D) structures. In this planar configuration, the electromagnetic energy is concentrated in a small region in the resonator plane, and they are often designed to achieve high *local* fields to ensure strong interactions with their immediate environment. This strategy has been used to develop metamaterial-based modulators[1] and to explore devices in the strong-coupling regime between light and matter.[4]

An important question is the possibility of importing this freedom from the diffraction limit into the realm of optoelectronic devices. Solving this problem is of fundamental and applied importance as it can lead to new operating principles and also enable applications. Semiconductor optoelectronic devices are typically fabricated in the *vertical* direction, with typical growths of a few microns using epitaxial techniques. Their artificially engineered nature has enabled, for instance, the development of lasers and detectors in difficult spectral ranges, such as quantum cascade (QC) lasers[9,10] and quantum-well infrared photodetectors (QWIP).[11] The aforementioned planar LC resonators do not suit these applications, as the former mostly operate in TE (transverse-electric) polarization, which does not couple with the gain medium of a QC laser or a QWIP detector that function in TM (transverse magnetic) polarization.

THz semiconductor devices mostly rely on metal-metal geometries. The active region (AR) is sandwiched between two metallic planes, ensuring operation in TM polarization, very good field confinement within the AR,[5] and a *vertical* size that can be deeply subwavelength[12–15] thanks to the lack of frequency cutoff for TM modes. However, the *longitudinal* size of cavities obtained with this architecture (*patch cavities*[16] or *transmission line resonators*[17]) is constrained by the diffraction limit, as intuitively shown in Fig. 1(a). It is not possible to implement patch cavities smaller than $\lambda_{\text{eff}}/2$ *in all three dimensions* (λ_{eff} is the wavelength within the active semiconducting region), and their resonance frequency can be tuned only via their lateral size.[13] These limitations arise because patch resonators are true photonic cavities, sustaining oscillations solely due to the time-varying electromagnetic field between the two conductors (the $\partial\mathbf{D}/\partial t$ term in the Ampère-Maxwell equation).[18]

Recently there have been proposals to convert the patch cavities of active THz devices into diffraction-free LC resonators, either by keeping a planar geometry[19–21] or by adopting a fully three-dimensional (3D) design.[22] However, some of these demonstrations were made with devices having a size comparable to half the wavelength, thus still in the diffraction limit. Furthermore, none of these works have shown that inductance and capacitance can be tuned separately as in an electronic circuit. The importance of answering these questions goes beyond a simple proof-of-principle. The development of truly hybrid electronic-photonic resonators—thanks to their subwavelength size—would enable practical devices. Examples are THz detectors with negligible dark current (since this latter scales with the device dimension), and also electronic-circuit tunable lasers.

In this Rapid Communication we demonstrate that only structures incorporating an inductance via at least one metallic loop can be endowed with the functionalities of a resonant electronic circuit, i.e., (i) truly subwavelength dimensions in all directions of space, and (ii) possibility of setting the resonance frequency by an independent capacitive/inductive load.

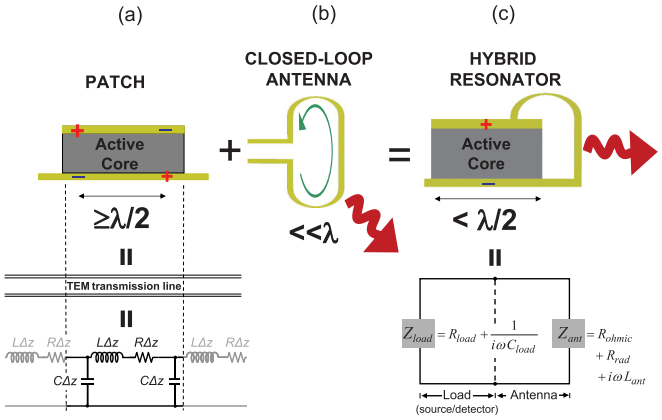

FIG. 1. (Color online) (a) Standard patch cavities consist of two metallic conductors sandwiching a dielectric core. They sustain purely photonic modes constrained by the diffraction limit. This limitation can be understood by noticing that a patch cavity is a section of transmission line: It cannot carry any power if the mode cannot oscillate along at least one direction of space. (b) A loop antenna couples with free space even if it is much smaller than the wavelength. (c) By combining a diffraction-limited patch cavity with a loop antenna, one obtains a subwavelength hybrid resonator. The excitation of the fundamental resonance is mediated by a real electric current in the antenna, freeing the device from the diffraction limit. Equivalently, the hybrid resonator can be seen as a loop antenna with a capacitive load formed by the two metallic plates.

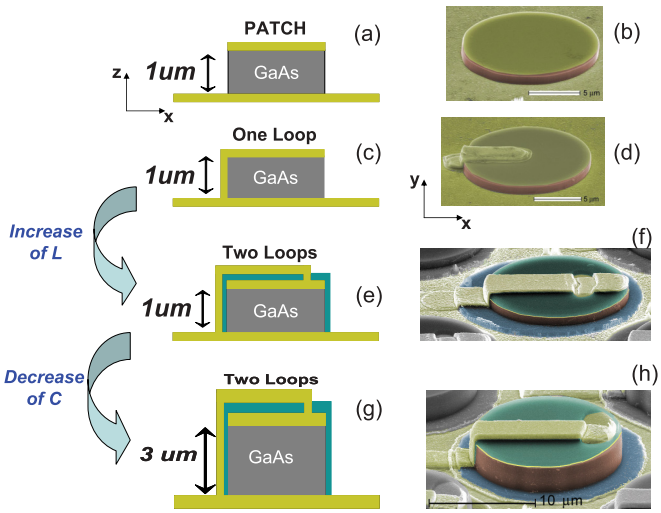

FIG. 2. (Color online) (a) and (b) Scheme and SEM image of a patch cavity with a 1-μm-thick semiconducting core (undoped epitaxial GaAs) sandwiched by gold layers. Connecting the two metal planes with a Au loop, one obtains a hybrid resonator freed from the diffraction limit (c) and (d). (e) and (f) A second metallic loop is added to increase L. (g) and (h) A thicker semiconducting core decreases C. The SEM images [(b), (d), (f), and (h)] have been colored to reveal the different material used: yellow = Au, pink = GaAs, and blue = SiO_2.

In the case of QCL- and QWIP-compatible cavities (i.e., structures derived from the patch geometry) the addition of a metallic loop requires a three-dimensional design. Figure 1(c) shows the scheme for such a hybrid resonator. The geometry is reminiscent of vertical split ring resonators developed for metamaterials[23] (or *shorted patch cavities* used in microwave engineering[24,25]): It can be seen as a closed-loop antenna [Fig. 1(b)] with a capacitive load.

Figure 2 summarizes the realized resonators. Figures 2(a) and 2(b) display a typical patch cavity which is used as a reference photonic device. The other panels show the schematics and corresponding SEM images of the new hybrid structures. In all this work, the core of the cavities is epitaxial undoped GaAs. Note that the hybrid resonators' 3D architecture is obtained with simple steps based on 2D lithography.[26] For each device family, different diameters have been implemented. The electrical connection between the opposing metallic plates—which is also the antenna, see Fig. 1(c)—forces the energy exchange via an electronic current. The fundamental resonance is now the configuration where the plates have electric charges with opposite signs [scheme in Fig. 1(c)], i.e., the electric field distribution has no nodal lines.

The principle of frequency tuning is also highlighted in Fig. 2: Adding a loop to the circuit increases the antenna inductance, with almost no effect on the capacitance. All dimensions equal, the two-loop resonator will therefore have a lower operating frequency owing to the increased inductance. It is also possible to act on the capacitance, as shown in Fig. 2(g): An increase in device thickness leads to a capacitance reduction, hence blue shifting the resonator frequency. This principle is supported by a simple model given in the Supplemental Material.[26]

The characteristic resonances of the system can be probed by reflectivity experiments.[13] The measurements were performed with a Fourier transform infrared spectrometer (FTIR) and a THz time-domain spectroscopy setup[27] (for frequencies below 1.5 THz). Owing to the spot size of the THz beam that is much larger than individual resonators, we fabricated arrays of closely spaced cavities intercepting the full section of the beam to maximize the contrast of the reflectivity measurements. Figure 3(a) describes the experimental geometry. The period is largely subwavelength to forbid all the diffractive orders except the 0th-order reflection. The sample bears geometrical similarities with metamaterials,[23] but we emphasize that our purpose is to engineer the resonant properties of the individual unit cell, and not the effective material properties that may arise at the macroscopic scale. We would not obtain more information measuring one single device.

Figure 3(b) shows the spectra obtained on the hybrid resonators of Fig. 2(h) (3-μm thick, two loops), for five different diameters, from 7 to 14 μm. Measuring devices with different diameters is useful to follow the resonances, hence simplifying their identification. The black curve (7 μm diameter)—acquired with a FTIR spectrometer—permits us to probe the full 1.5–9 THz range. Two resonances are observed. The lower frequency dip ($f \approx 2.6$ THz) corresponds to the fundamental oscillation mode, whose electric field distribution [z component, see inset of Fig. 3(b)] has no nodal lines.[22] This mode, thanks to the current loop, has a net magnetic moment along the y direction so it couples, even at normal incidence, with electromagnetic waves with a nonzero magnetic field component along the y axis. The higher energy mode ($f \approx 7$ THz) is instead the standard dipolar mode of

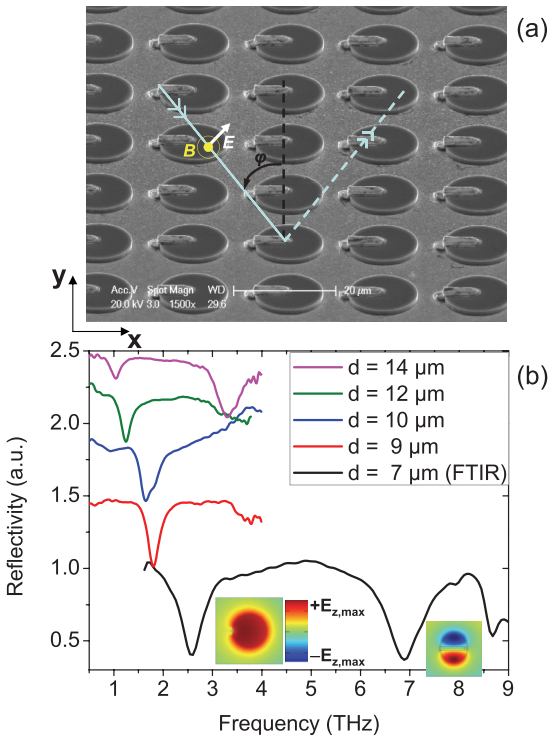

FIG. 3. (Color online) (a) SEM image of a typical sample and scheme of the geometry for reflectivity measurements. (b) Reflectivity spectra for hybrid resonators of the type of Fig. 2(h) and diameters ranging from 7 to 14 μm. The smallest structure has been measured using an FTIR interferometer. The other curves were obtained with a THz TDS setup.[27] The data are vertically offset to highlight the resonance position. The reflectivity baseline is $\approx$0.9 for all devices. Insets: Simulated cross section of the vertical component of the electric field for the fundamental mode (left) and the first higher-order mode, i.e., the dipolar resonance also excited in standard patch cavities (right). The field patterns have been computed using commercial code.

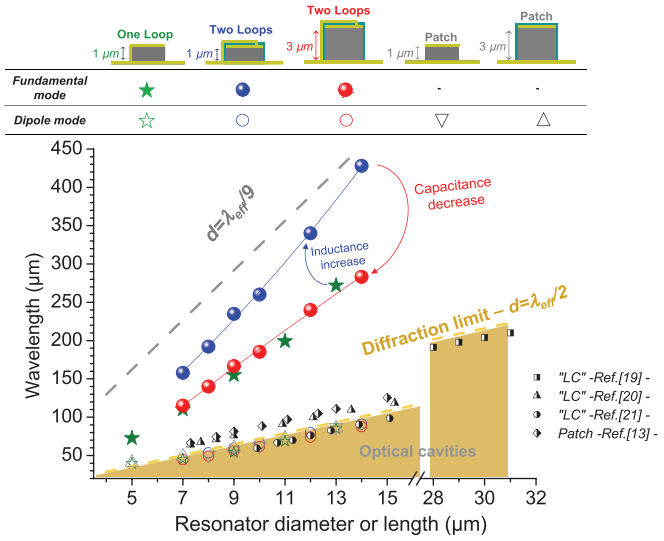

FIG. 4. (Color online) Effective wavelength of the fundamental mode λ_{eff} vs device diameter D for one-loop resonators with a 1-μm-thick core (green stars), two-loop resonators with a 1-μm-thick core (blue dots), and two-loop resonators with a 3-μm-thick core (red dots). The dashed lines are guides for the eyes indicating the $d = \lambda_{\text{eff}}/2$ and $d = \lambda_{\text{eff}}/9$ dependencies. Also shown is the spectral position of the dipolar mode as a function of D for all the structures considered here (open symbols: stars, circles, and triangles). The top part is a complete legend of the fabricated and measured devices. The black symbols are data extracted from the literature for "LC" cavities (Refs. 19–21) and standard square patch cavities (Ref. 13). References 13 and 21: 0.8-μm-thick devices; Ref. 20: 1.5-μm thick; and Ref. 19: 8-μm thick.

patch cavities corresponding to the $\lambda_{\text{eff}}/2$ condition, where λ_{eff} is the wavelength *inside* the material. The electric field distribution features a nodal line, hence the charge oscillation takes place *within* each opposing plate, and the lateral electrical connection plays no role.

The other data in Fig. 3(b) are acquired with a THz-TDS setup, whose useful bandwidth can extend to lower frequencies, from $\sim$0.3 to $\sim$4 THz, and is thus ideally adapted to probe the lower frequency resonances. The fundamental resonance can be followed, down to $\approx$1 THz for a $d = 14$ μm cavity, which corresponds to $\lambda_{\text{eff}}/6$ confinement. The higher frequency dipolar resonance is cut off by the bandwidth of the TDS system, except for the largest resonator ($\sim$3.4 THz, purple curve).

Figure 3(b) allows one to extract the Q factors. The fundamental magnetic resonances have Qs of the order of $\sim$7, while the dipolar resonances (the standard *patch cavity* modes) exhibit Qs of $\sim$10. This latter value is in agreement with the literature on metallic patch cavities operating in the THz range,[13,14,19–21] with Qs dominated by the ohmic losses. Indeed metals are good conductors in the THz, but here the extreme thinness of the active region ($\sim$1–3 μm) with respect to the wavelength (100 to 400 μm) leads to substantial field penetration in the metallic regions, and thus to loss. Such losses are however not incompatible with lasing, as demonstrated in Ref. 12.

A summary of all the reflectivity measurements is reported in Fig. 4, which is the core result of the paper. It reports the wavelength of the modes of *all* the resonators as a function of cavity diameters d (green, blue, and red symbols). The dark yellow dotted line marks the diffraction limit of photonic resonators ($\lambda_{\text{eff}} = 2d$). The measured fundamental magnetic resonances (full green, blue, and red symbols) largely break this limit: A maximum confinement up to $\lambda_{\text{eff}}/9$ *in all the three dimensions*[28] is obtained in the case of the two-loop/1-μm-thick device. The effective volumes achievable are also record low: The $d = 14$ μm and 1-μm-thick two-loop device operates at $\lambda \approx 450$ μm, which corresponds to an effective volume $V_{\text{eff}} = 6 \times 10^{-4}(\lambda/2n_{\text{eff}})^3$.

The fundamental frequency of the hybrid resonators is set by the external circuit. The difference between green and blue symbols mainly stems from an *inductance* increase since only a current loop is added to the hybrid resonators. Two-loop devices are found to operate at lower frequencies, correctly following the $f \sim 1/(LC)^{1/2}$ rule of LC circuits. In turn, the difference between blue and red symbols mainly originates from a *capacitance* decrease of a factor of 3 (the active region thickness is increased from 1 to 3 μm). This leads to a frequency *increase* of $\sim\sqrt{3}$, which is correctly experimentally measured.

These results are in strong contrast with the dipolar modes (open color symbols in Fig. 4)—the standard ground state eigenvalues of purely photonic resonators[13]—that are *strictly* constrained by the diffraction limit (with $n_{GaAs} = 3.6$) and therefore lay on the $\lambda_{eff}/2$ line independently of cavity type or active-core thickness.

We have experimentally demonstrated that these resonators do indeed possess two key functionalities of an electronic oscillator: extremely subwavelength size and frequency set by a circuit. Furthermore, they ensure a very good field confinement within the AR, necessary for device applications. We now argue that a three-dimensional design is necessary to create hybrid electronic-photonic patch cavities. To this end, we compare their properties with a seemingly related design which has been used in QC lasers and QED-polaritonic experiments.[19–21]

The cavity geometry of Refs. 19–21 is made of two small conducting patches connected *in the same plane* by a thin metallic wire. In this design, a current loop can form between the ground and top planes through the displacement currents $\partial \mathbf{D}/\partial t$ only. The system can thus also be seen as a combination of inductive elements (the top metallic surfaces) and capacitive regions (the gaps between the conducting patches and the ground plane). To verify whether such a combination of L and C components is free from the diffraction limit, we have compiled the resonance frequency of the experimental samples of Refs. 19–21 (as extracted from the figures) as a function of their longitudinal size (black symbols in Fig. 4). The figure shows that all the cavities are parallel to the $\lambda_{eff}/2$ line, independent of the sample thickness and/or patch shapes (squares, rounds, half-rounds). In other words, they seem to support purely photonic modes.

Before commenting on this behavior, we note that these structures are composed of two coplanar metallic sheets, and therefore they are equivalent to a finite length of transmission line [Fig. 1(a)]. If fringing fields effects are neglected, the ground state resonance of transmission line resonators can be approximated as

$$f \approx \frac{1}{2\sqrt{L \cdot C}}. \tag{1}$$

Since the fundamental theorem of transmission lines[17] links inductance (L') and capacitance (C') per unit length ($L' \cdot C' = 1/c^2$, where c is the speed of light), they *cannot* be independently adjusted. Quick algebra using Eq. (1) shows that this constrains the device to the diffraction limit (Fig. 4, dark yellow dotted line). In this sense, these cavities are not fundamentally different from standard patch resonators. To corroborate this claim, we have also added on Fig. 4 the characteristics of a few patch cavities considered in the recent literature[13]: These structures also follow the $\lambda_{eff}/2$ line, as expected.[29]

The hybrid resonators of Fig. 3—thanks to their 3D character—bypass this fundamental constraint and effectively disentangle capacitance and inductance because transmission line theory and its fundamental theorem cited above only applies to topologies equivalent to the parallel plate geometry. Their behavior can be inferred with the well known formula from antenna theory:

$$Z_{ant} = Z^*_{load}, \tag{2}$$

with Z_{ant} as the antenna complex impedance, and Z^*_{load} as the complex conjugate of the load impedance[16] [Fig. 1(c)]. The imaginary part of Eq. (2) yields the resonance frequency and essentially reduces to an LC model. Given the extreme compactness of the resonators, it is difficult to precisely assign inductance and capacitance values (they lie approximately in the pH and fF ranges, respectively). While beyond the scope of this work, we nevertheless propose a basic model in Supplemental Material.[26] It yields a qualitative agreement with the trend of the experimental data, confirming the main results of this Rapid Communication.

Finally, one can wonder why the distinction between planar and three-dimensional geometries does not apply at higher frequencies. It is known that parallel metallic cut wires can act as highly subwavelength LC resonators in optics.[30] The difference arises from the dielectric function of metals at high frequencies. Regardless of their geometry, metallic wires at optical frequencies support localized surface plasmon resonances with deep subwavelength confinement. But at THz frequencies, very far from the plasma frequency, it is the topology which sets the physical length of the device, while the material parameters play a very minor role.

The hybrid resonators presented in this work can lead to applications for lasers and detectors: Their size can be defined *by design*, acting on the electronic section of the resonator which behaves as an antenna element. A wide variety of antennas (dipoles, butterfly, broadband) is available to target specific applications. In combination with detector active regions, this can lead to THz QWIP detectors with extremely small dark currents. Predicting and optimizing the emissive properties of these devices using formalism based on complex impedances would be a major step forward and represents one of the immediate perspectives of this work.

We thank J.-J. Greffet for useful discussions. We acknowledge financial support from the French National Research Agency (ANR-09-NANO-017 “Hi-Teq” and ANR-09-NANO007 “GOSPEL”), and from the Triangle de la Physique (Project “PHLARE”). The device fabrication has been performed at the nano-center CTU-IEF-Minerve, which was partially funded by the Conseil Général de l’Essonne.

*aloyse.degiron@u-psud.fr

†raffaele.colombelli@u-psud.fr

[1] H. T. Chen, J. F. O’Hara, A. K. Azad, A. J. Taylor, R. D. Averitt, D. B. Shrekenhamer, and W. J. Padilla, Nat. Photon. **2**, 295 (2008).

[2] B. Reinhard, O. Paul, R. Beigang, and M. Rahm, Opt. Lett. **35**, 1320 (2010).

[3] G. Scalari, C. Maissen, D. Turčinková, D. Hagenmüller, S. De Liberato, C. Ciuti, C. Reichl, D. Schuh, W. Wegscheider, M. Beck, and J. Faist, Science **335**, 1323 (2012).

[4] D. Dietze, A. Benz, G. Strasser, K. Unterrainer, and J. Darmo, Opt. Express **19**, 13700 (2011).

[5]K. Unterrainer, R. Colombelli, C. Gmachl, F. Capasso, H. Hwang, D. L. Sivco, and A. Y. Cho, Appl. Phys. Lett. **80**, 3060 (2002).
[6]A. G. Davies, A. D. Burnett, W. H. Fan, E. H. Linfield, and J. E. Cunningham, Nat. Mater. **11**, 18 (2008).
[7]M. Tani, S. Matsuura, K. Sakai, and S.-I. Nakashima, Appl. Opt. **36**, 7853 (1997).
[8]J. B. Pendry, A. J. Holden, D. J. Robbins, and W. J. Stewart, IEEE Trans. Microwave Theory Tech. **47**, 2075 (1999).
[9]J. Faist *et al.*, Science **264**, 553 (1994).
[10]R. Köhler *et al.*, Nature (London) **417**, 156 (2002).
[11]J. C. Cao and H. C. Liu, in *Advances in Infrared Photodetectors*, Semiconductors & Semimetals, Vol. 84 (Academic, New York, 2011).
[12]E. Strupiechonski, D. Grassani, D. Fowler, F. H. Julien, R. Colombelli, S. P. Khanna, Lianhe Li, E. H. Linfield, A. G. Davies, and A. B. Krysa, Appl. Phys. Lett. **98**, 101101 (2011).
[13]Y. Todorov, L. Tosetto, J. Teissier, A. M. Andrews, P. Klang, R. Colombelli, I. Sagnes, G. Strasser, and C. Sirtori, Opt. Express **18**, 13886 (2010).
[14]Y. Todorov, A. M. Andrews, I. Sagnes, R. Colombelli, P. Klang, G. Strasser, and C. Sirtori, Phys. Rev. Lett. **102**, 186402 (2009).
[15]P. Jouy, Y. Todorov, A. Vasanelli, R. Colombelli, I. Sagnes, and C. Sirtori, Appl. Phys. Lett. **98**, 021105 (2011).
[16]C. A. Balanis, in *Antenna Theory: Analysis and Design*, 2nd ed. (Wiley, New York, 1996).
[17]D. H. Staelin, A. W. Morgenthaler, and J. A. Kong, in *Electromagnetic Waves* (Prentice Hall, Englewood Cliffs, NJ, 1993).
[18]Ampere-Maxwell equation: $\nabla \wedge \mathbf{H} = \mathbf{J} + \frac{\partial \mathbf{D}}{\partial t}$.
[19]C. Walther, G. Scalari, M. Amanti, M. Beck, and J. Faist, Science **327**, 1495 (2010).
[20]M. Geiser, C. Walther, G. Scalari, M. Beck, M. Fischer, L. Nevou, and J. Faist, Appl. Phys. Lett. **97**, 191107 (2010)
[21]M. Geiser, F. Castellano, G. Scalari, M. Beck, L. Nevou, and J. Faist, Phys. Rev. Lett. **108**, 106402 (2012).
[22]E. Strupiechonski, G. Xu, M. Brekenfeld, Y. Todorov, N. Isac, A. M. Andrews, P. Klang, C. Sirtori, G. Strasser, A. Degiron, and R. Colombelli, Appl. Phys. Lett. **100**, 131113 (2012).
[23]K. Fan, A. C. Strikwerda, H. Tao, X. Zhang, and R. D. Averitt, Opt. Express **19**, 12619 (2011).
[24]R. Waterhouse, Electron. Lett. **37**, 604 (1995).
[25]R. Porath, IEEE Trans. Antennas Propag. **48**, 41 (2000).
[26]See Supplemental Material at http://link.aps.org/supplemental/10.1103/PhysRevB.87.041408 for calculation of the system resonance frequency with an *LC* model, numerical simulations of the electromagnetic field distribution, and device fabrication.
[27]S. Kono, M. Tani, and K. Sakai, in *Terahertz Optoelectronics*, edited by K. Sakai (Springer, Berlin, 2005), Chap. 2.
[28]The confinement is actually much more in the vertical direction, but this is just a trivial consequence of the lack of cutoff for TM modes in metal-insulator-metal waveguides.
[29]The data points of the standard patch resonators[13] and those of Ref. 20 are slightly above the $\lambda_{\text{eff}}/2$ line because of fringing field effects, which arise because the very thin semiconducting layer of these structures has not been etched.
[30]V. M. Shalaev, W. Cai, U. K. Chettiar, H.-K. Yuan, A. K. Sarychev, V. P. Drachev, and A. V. Kildishev, Opt. Lett. **30**, 3356 (2005).